Full paper

Actuation and sensor integrated self-powered cantilever system based on TENG technology

Jie Chen[a,b,1], Hengyu Guo[a,c,1], Zhiyi Wu[a,1], Guoqiang Xu[d], Yunlong Zi[d], Chenguo Hu[b,**], Zhong Lin Wang[a,c,*]

[a] School of Materials Science and Engineering, Georgia Institute of Technology, Atlanta, GA, 30332, USA
[b] Department of Applied Physics, State Key Laboratory of Power Transmission Equipment and System Security and New Technology, Chongqing University, Chongqing, 400044, PR China
[c] Beijing Institute of Nanoenergy and Nanosystems, Chinese Academy of Sciences, Beijing, 100083, PR China
[d] Department of Mechanical and Automation Engineering, The Chinese University of Hong Kong, Shatin, N.T., Hong Kong, China

ABSTRACT

Actuation and sensors for driving and monitoring of cantilever beam system are of most significant in the field of micro-electro-mechanical systems (MEMS). However, the AC voltage driving module and piezoelectric materials used in cantilever highly raise the system complexity and costs. Here, we propose a motion-triggered cantilever beam (MC) accompanied by an integrated real-time oscillation-monitoring sensor (ROS) designed based on the principle of triboelectric nanogenerator (TENG). Utilizing the periodically built and neutralized high DC voltage during the operation of the freestanding mode TENG, the low-frequency mechanical motion (down to 5 up to 200 mm/s) can be converted into high-frequency oscillation up to 100 Hz. Different from AC trigger method that requires excitation frequency matching the intrinsic frequency of the cantilever, DC actuation strategy is universal to all kinds of cantilever systems. Additionally, based on the single electrode mode TENG, the integrated self-powered ROS shows ultra-high sensitivity (223 mV/mm compared with 72 mV/mm for laser micro-motion meter). Finally, a self-powered micro-weighing system based on MC and ROS is demonstrated. This work exhibits notable advantages of using TENG technology for both power supply and sensing in MEMS applications.

1. Introduction

The cantilever beam is a ubiquitous structure in the field of micro-electro-mechanical systems (MEMS) [1–3]. Utilizing the resonant frequency shift, cantilevers have been widely used in environmental monitoring [4,5], gravimetric analysis [6,7] and surface/bulk stress measurement [8–10]. In general, to measure the frequency changes of cantilevers, the first step is to actuate it by a perturbing driving force. Second, the resulting vibration must be recorded for post-processing by a read-out technique. Typically, a cantilever is excited by an AC voltage, working with an active piezoelectric layer clinging to the cantilever beam tightly [11,12]. The corresponding binding-induced changes in cantilever oscillation frequency are detected by the optical leverage [13], resistance meter [14], piezoelectric [8,9] and piezoresistive sensor [11,15]. However, this structure not only increases the energy consumption for the cantilever vibration actuation and

detection, but also augments the fabrication cost for functional materials usage, and it even reduces the system integration level caused by peripheral circuits and sensing elements. To solve the above problems, a self-powered technology is highly desired for the cantilever actuating and monitoring integrated system. Typically, the components in a self-powered system operate independently, sustainably and wirelessly without an external energy supply [16], which has a great potential for working as both excitation source and vibration monitor of a cantilever.

Over the past seven years, the triboelectric nanogenerator (TENG) [17], based on the contact electrification and electrostatic induction, has been proved to be one of the most effective technology to harvest mechanical energy in low-frequency region [18,19], with unique merits of easy-fabrication, low-cost, material-diversity, portability. Moreover, TENG can easily produce high open-circuit voltage up to several thousand volts, which has been applied for the nano-electrospray ionization [20,21], micro-plasma generation [22], microfluidics transport

fields [23,24], indicating that TENG has a capability to work as a high voltage source. In addition, TENG can convert a micro-mechanical motion into an electric output signal, that is to say, this technology can be used to directly detect a dynamic mechanical motion without applying a power source to the device [25–28]. Recently, various TENG-based devices for detecting micro-motion have been developed, such as, eye motion-triggered self-powered mechnosensational communication system [29], the breathing-driven implanted device [30,31], alcohol breath analyzer [32,33], heartbeat and respiration monitor [34,35], and artificial cochlear [36,37]. Compared with the traditional sensors, TENG-based self-powered sensors have characteristics of high sensitivity, high signal-to-noise-ratio and multifunction. Thus, with the strength of TENG, it is promising to design and fabricate a self-powered and self-sensing cantilever-based system.

In this work, we propose and realize a motion-triggered cantilever beam (MC) accompanied by an integrated real-time oscillation-monitoring sensor (ROS) based-on triboelectric nanogenerator (TENG) technique. The cantilever with a trigger electrode connected to TENG can build and neutralize the high DC voltage periodically, and thus keeps a relatively stable and high-frequency oscillation when applying a low-frequency mechanical motion on TENG. The oscillation performance of MC is systematically studied at various factors, including the cantilever size (length, width), trigger electrode width, position (parallel and vertical direction to the cantilever) and the operation speed of TENG. From the experimental results, the low-frequency mechanical motion (down to 5 mm/s up to 200 mm/s) can be converted to the stable and high-frequency oscillation up to 100 Hz. For the sensing component, utilizing the single electrode mode TENG, a real-time oscillation-monitoring sensor (ROS) with high integratability and low-cost is fabricated and it shows a much higher sensitivity of 223 mV/mm compared with a laser micro-motion sensor (Panasonic HG-C1100, 72 mV/mm). Furthermore, the designed MC system is demonstrated for a self-powered micro-weighing system, in which the mass of an object can be precisely detected just by hand sliding. This work exhibits a prospective strategy of using TENG technology for power source and sensing applications in a self-powered MEMS.

2. Results and discussion

2.1. Working principle of motion-triggered cantilever beam

Traditionally, the cantilever excited by AC electric field requires the voltage frequency matching the cantilever's intrinsic resonance frequency. Therefore, only an AC electric field involving varying frequencies could meet the demands of different parameter cantilever systems. In this work, we propose a DC actuation strategy which has the universality for cantilever systems with different resonant frequencies. Moreover, benefit from the high voltage generated from triboelectric nanogenerator (TENG), a low-frequency and random motion-triggered cantilever beam (MC) can be obtained for achieving a high-frequency and regulated oscillation. The system structure is illustrated in Fig. 1a, including a free-standing mode TENG and a one-end fixed steel cantilever with a trigger electrode. When the high DC output voltage from TENG is applied between the cantilever and trigger electrode, the cantilever can be excited and then keeps a stable oscillation. Measured open-circuit voltage and short-circuit transfer charges of the free-standing mode TENG under different operation speeds, and the simulated potential distribution are presented in Fig. S1. The corresponding digital photograph of the experimental apparatus is shown in Fig. 1b. The detailed fabrication process is presented in materials and methods.

The basic principle of DC voltage actuated cantilever is to periodically introduce energy replenishment during the damped oscillation process. Fig. 1c displays the working process and charges distribution of MC. It is known that, after interacting with nylon, PTFE can retain a layer of negative bound charges that do not dissipate in a long time [38]. Before the MC starts working, the nylon slider and the un-covered

electrode are positively charged due to the electrostatic induction effect (initial state). Later, moving the slider changes the overlapped electrode area, therefore, opposite charges will flow from the two electrodes to the cantilever and the trigger electrode respectively, and reach a new electric equilibrium. At the same time, the accumulated opposite charges between the cantilever and trigger electrode would attract each other, leading to the deformation of the cantilever (I). Continuing to move the slider, more and more charges would flow to the cantilever and trigger electrode and thus increase the electric field until discharge happens in a closer distance (II). The cantilever starts oscillation in the form of damped vibration owing to air friction. The measured oscillation curves of the above three stages are presented in Fig. S2a. By operating TENG continuously, the electric field between the cantilever and trigger electrode will be re-established to realize a new discharge point (III). During the electric field periodically building and neutralizing process, the cantilever keeps a stable oscillation (Fig. S2b). Fig. 1d simulates the electric field distribution and cantilever deformation when a high voltage is applied to the trigger electrode. The photographs of the MC working process are recorded by a high-speed camera, shown in Fig. 1e–i. The entire oscillation process is presented in Video S1.

Supplementary video related to this article can be found at https://doi.org/10.1016/j.nanoen.2019.103920.

2.2. Factors on DC voltage actuated cantilever

As a new actuation strategy, we systematically investigate the various parameters that could affect the oscillation performance of the cantilever. Fig. 2a is the scheme of the experimental setup, including a high voltage source, a grounded cantilever beam, and a laser micro-motion meter. The photograph of the apparatus is shown in Fig. S3. For the free vibration, the measured eigenfrequency of the cantilever (length: 50 mm, width: 5 mm, thickness: 100 μm) is 28.04 Hz, in the form of damping oscillation (Fig. 2b). When applying 1.5 kV voltage on the trigger electrode, a stable oscillation with 27.95 Hz frequency can be monitored (Fig. 2c). By changing the DC voltage applied on the trigger electrode, unstable oscillation appears when voltage up to 2.5 kV (Fig. S4). These results indicate that a proper DC voltage can actuate the cantilever beam in a stable state, and the oscillation frequency shift is within 1%. However, excessive rising actuated voltage is not conducive to maintaining a stable oscillation. Next, the effects of the trigger electrode width, position, and cantilever size on oscillation performance are studied. Fig. 2d depicts the influence of the electrode width on oscillation's turn-on voltage, amplitude, and frequency (other parameters are fixed, including the electrode position X: 1 mm, Y: 40 mm and cantilever length: 40 mm, width: 5 mm, thickness: 100 μm). It should be noted that the turn-on voltage is the minimum voltage that actuates the cantilever. With the electrode width increasing up to 5 mm, the amplitude, and frequency almost keep constant, while the turn-on voltage decreases gradually, as the wider trigger electrode forms a larger electric field area, leading to a larger electrostatic force under the same applying voltage. Thus, a lower turn-on voltage is required to actuate the cantilever with a wider trigger electrode. The simulated electric field distribution and cantilever deformation with different electrode width under a constant voltage are simulated in Fig. S5. In addition, the relationship between the electrode position and oscillation performance is also tested (other parameters are fixed, including the electrode width: 1.5 mm, cantilever length: 80 mm, width: 5 mm, thickness: 100 μm). With the electrode close to the fixed end (Y position from 80 mm to 20 mm) or far away from the cantilever (X position from 0.5 mm to 2.5 mm), the shift of oscillation frequency is not obvious; when both the turn-on voltage and amplitude increase (Fig. 2e and f). When the electrode is close to the fixed end, the arm of force reduces. Thus, a greater force is required to break the cantilever's balance state according to the lever principle. As illustrated in Fig. 2f insect, the angle between the electrode and the fixed end of the cantilever increases with
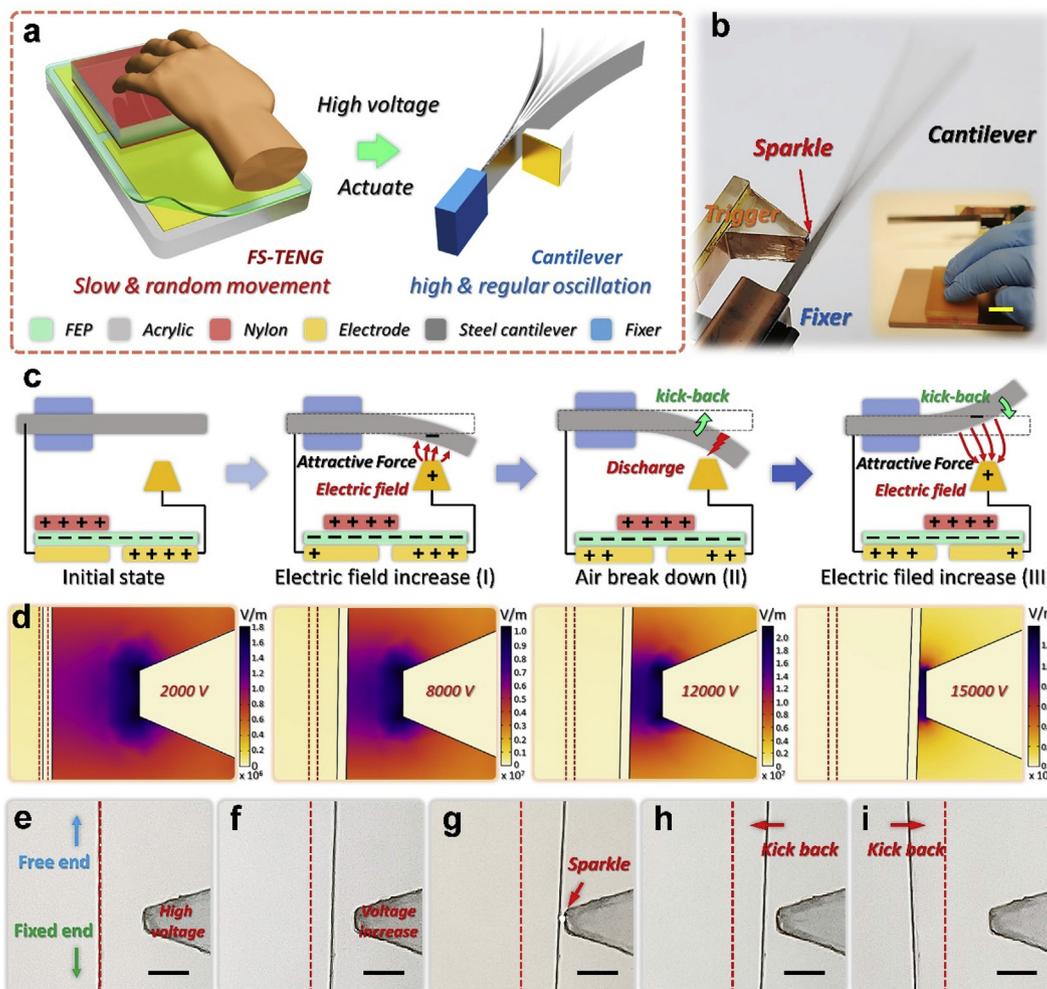
Fig. 1. Schematic illustration and working mechanism of the motion-triggered cantilever beam (MC). a) Structural scheme of the free-standing mode triboelectric nanogenerator (produce high output voltage when applying a slow and random mechanical motion) and the DC voltage actuated cantilever beam (form high and regular oscillation when supplying a high DC voltage). **b)** Digital photograph of the cantilever driven by sliding the triboelectric nanogenerator. Scale bar: 2 cm. **c)** Actuating mechanism of the cantilever beam and the corresponding charge distribution scheme of triboelectric nanogenerator. **d)** Simulated electric field distribution and cantilever deformation when applying different high voltages. **e)-i)** High-speed camera captured working process of the DC voltage actuated cantilever beam.

the electrode away from the cantilever, therefore, the amplitude at the free end gets/becomes bigger. The waveforms of the above experiments are shown in Figs. S6–S8.

After that, the effect of cantilever size (length and width) on the oscillation performance is also investigated to demonstrate the universality of the DC voltage actuation strategy (Figs. S9–S11). From Fig. 2g, with diminishing of the cantilever length from 80 mm to 20 mm, the turn-on voltage increases from 0.4 kV to 7.5 kV, and the oscillation frequency rises from 11.096 Hz to 153.199 Hz. Compared with the eigenfrequency of free oscillation under the gravitational field (solid line in Fig. 2g bottom and curve in Fig. S10), the measured frequency of the cantilevers with different lengths has a small deviation caused by the synergy effect between the electric field and gravitational field. From Fig. 2h, with augmentation of the cantilever thickness, both the turn-on voltage and frequency increase. Moreover, compared with the single trigger electrode, the double side trigger improves the symmetry of the amplitude without a large frequency shift (Fig. 2i). From the above experimental results, this DC voltage actuation strategy is feasible and suitable for various cantilever systems.

2.3. Performance of motion-triggered cantilever beam

In order to realize a motion-triggered cantilever system, a free-

standing mode TENG is utilized in this work, due to its high output voltage during a random sliding movement. Fig. 3a shows the short-circuit charge transfer and open-circuit voltage curves of TENG with 110 mm × 175 mm dimension. In a half cycle, the TENG can generate the maximum 1.5 μC charges and 7.5 kV voltage respectively, which have a linear relationship with the sliding distance. Fig. 3b exhibits the schematic configuration of the motion-triggered cantilever, in which two electrodes of TENG are electrically connected to the trigger electrode and the fixed end of the cantilever. Utilizing the output of TENG to actuate the cantilever, the oscillation and charge transfer are monitored by the laser micro-motion meter and ampere meter, respectively. During the oscillation process, once the discharge happens between the cantilever and trigger electrode, a pulse current will be detected and the built voltage will be neutralized. With continuous movement of the slider of TENG, the voltage will be re-established and trigger the cantilever beam in the next cycle. Therefore, the cantilever can be actuated and keeps a stable oscillation by a sliding motion. Fig. 3c displays the simultaneously collected current and amplitude of a stable oscillation cantilever (length: 80 mm, width: 5 mm, thickness: 100 μm). From the enlarged inset in Fig. 3c bottom, once the amplitude reaches the negative maximum, discharge between the cantilever and electrode would happen, making the cantilever oscillating stable. However, decreasing the working speed of TENG to a certain value, after every discharge
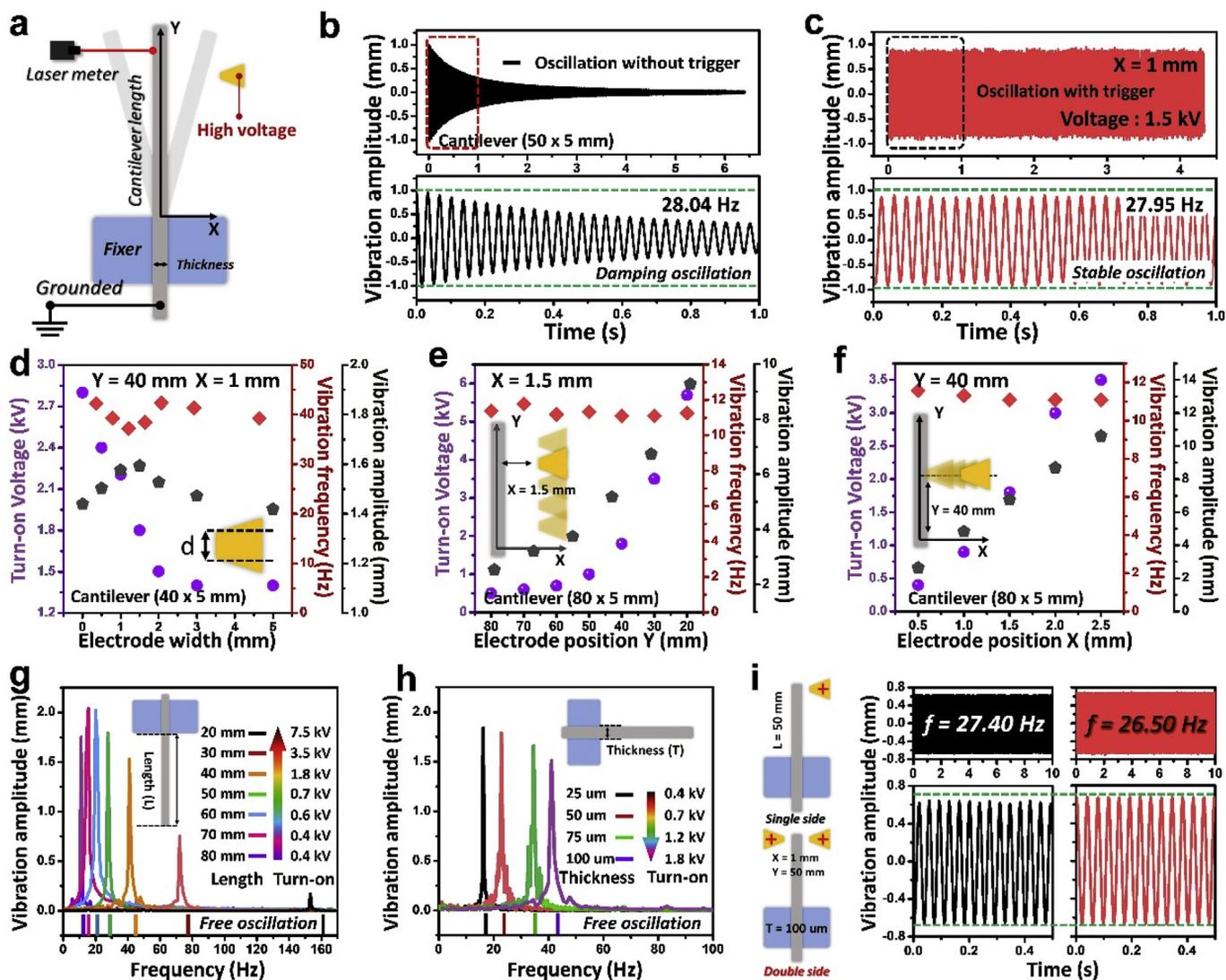
Fig. 2. Influential parameters on the oscillation performance of the DC voltage actuated cantilever beam. **a)** Scheme and controlled parameters of the experimental platform. **b)** Damping oscillation of the cantilever beam (length: 50 mm, width: 5 mm, thickness: 100 μm) without the DC voltage triggering. **c)** Stable oscillation of the cantilever beam with the DC voltage trigger (trigger position Y = 50 mm, X = 1 mm). **d)-f)** Turn-on voltage and oscillation property of the cantilever beam with different width, Y position and X position of the trigger electrode respectively. **g)-h)** Influence of cantilever length and thickness on the turn-on voltage and oscillation property, respectively. **i)** Oscillation performance comparison between the single side and double side DC voltage trigger.

occurs between the cantilever and trigger electrode, the cantilever is actuated, but, the oscillation amplitude gradually decreases. That is, the charge replenishment to the trigger electrode fails to sustain the stable oscillation state.

On the contrary, with a greater increase in the operation speed of TENG, the generated high voltage will result in an irregular discharge, disturbing the cantilever's oscillation. In both cases, it is difficult to realize stable oscillations. Therefore, a proper working speed range of TENG is required to achieve a stable oscillation of each cantilever system. Fig. 3d shows the working speed range of TENG and the corresponding oscillation states of a 40 mm length cantilever. In the damping area (the working speed of TENG from 1 mm/s to 35 mm/s), charges accumulate slowly, and the cantilever oscillates damply. When the velocity rises from 35 mm/s to 100 mm/s, the cantilever beam can oscillate stably on account of the proper charge replenishment. With continuously increasing TENG working speed, an unstable oscillation appears due to the irregular discharge. The whole oscillation processes of each state are recorded in Video. S2–S4. Based on the preceding experimental results, the turn-on voltage is related to the cantilever length and trigger electrode position (Fig. 2e–g). With the cantilever

length reduced, when the electrode is close to the fixed end (Y position decrease) or electrode away from the cantilever (X position increase), a greater turn-on voltage is required to activate the cantilever. As shown in Fig. 3e–g, we systematically investigate the relationship between the stable oscillation state of cantilever systems and TENG working speed under various conditions. For the cantilever system with a low turn-on voltage, TENG that operates at very low speeds can activate it. For a higher turn-on voltage cantilever system, it can oscillate stably within a larger TENG operation speed range. The corresponding oscillation waveforms of various parameters cantilever systems at each oscillation state are exhibited in Figs. S12–S14. From all the results in this part, the motion-triggered cantilever systems with different parameters can be achieved via TENG technology.

Supplementary video related to this article can be found at https://doi.org/10.1016/j.nanoen.2019.103920.

2.4. Integrated tribo-sensor for real-time oscillation monitoring

Traditionally, the oscillation of a cantilever is detected by optical leverage and piezoelectricity. However, the valid signal of piezoelectric
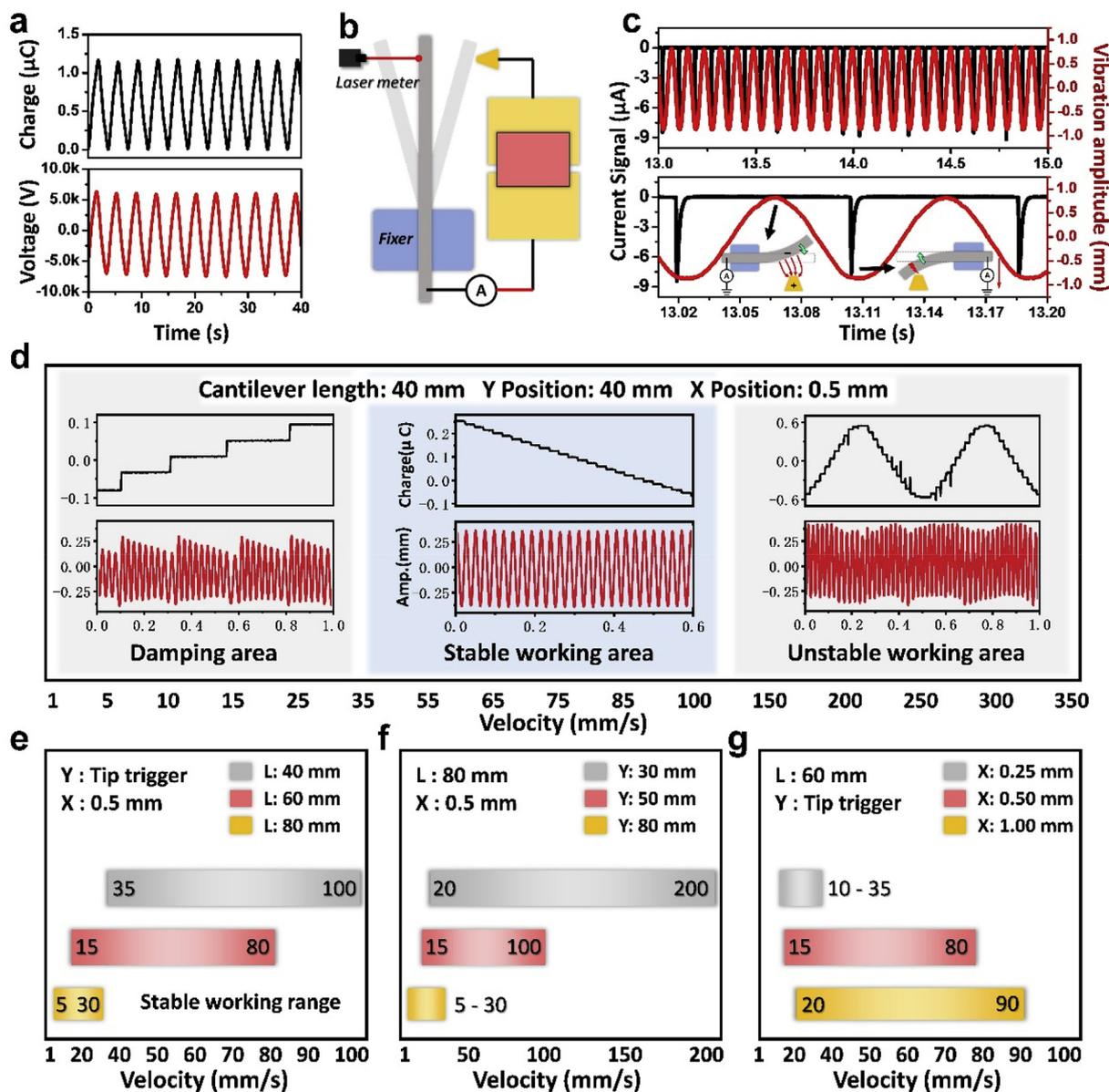
Fig. 3. Oscillation performance of the cantilever beam actuated by triboelectric nanogenerator. a) Output charge and voltage of the free-standing mode triboelectric nanogenerator. **b)** Scheme of the experimental setup. **c)** Pulse current signal and synchronous oscillation curve recorded by the laser micro-motion meter. **d)** Oscillation performance of the cantilever beam driven by triboelectric nanogenerator under different working speeds. **e)-g)** Influence of the cantilever length, trigger position Y and X on the velocity range of triboelectric nanogenerator when the cantilever keeps stable oscillation, respectively.

technology is too small to be recognized from background noise, and the optical one is complicated. Based on the previous reports, TENG can be used as a sensor to directly detect a dynamic mechanical motion without a power supply, occupying high signal-to-noise rate and sensitivity. Therefore, we design a real-time oscillation-monitoring sensor (ROS) based on TENG technology. Fig. 4a depicts the experimental apparatus, in which a simple single-electrode mode TENG is employed on the other side of the beam to real-time monitor the oscillation of the cantilever. In order to avoid the disturbance caused by the periodically built and neutralized electric field during cantilever oscillation process, two symmetric electrodes are designed (EA and EB, shown in Fig. 4b). The reference electrode EB is specially introduced to capture the background noise. By attaching a tribo-layer to the cantilever corresponding to the EA position, the signal captured by the EA is the oscillation information with noise. Fig. 4c exhibits the simultaneously collected signals from EA and EB. By difference calculating the signals, the valid voltage can be obtained. Compared with the amplitude

detected by the laser micro-motion sensor, the voltage curve from EA-EB is a sinusoidal wave and well-matched to the signal from a laser sensor (Video. S5). Moreover, for different lengths of cantilevers, the error between the measured frequency from ROS and that from laser sensor is about 2% (Fig. S15), indicating that this newly designed ROS can replace a laser sensor to monitor cantilever oscillations.

Supplementary video related to this article can be found at https://doi.org/10.1016/j.nanoen.2019.103920.

For a sensor, sensitivity is an important factor for characterizing its performance. To characterize the performances of ROS, the output voltages under the different trigger and sensing positions are measured (Figs. S16–S17). As illustrated in Fig. 4d, with raising the trigger position (from 0.2 mm to 1.0 mm) or increasing the oscillation amplitude of the cantilever (from 0.618 mm to 2.055 mm), the output voltage from ROS linearly grows up to 166.4 mV. The sensitivity of this designed ROS is 223 mV/mm, while that of the used laser sensor is 72 mV/mm the corresponding calculation is shown in Fig. S18.
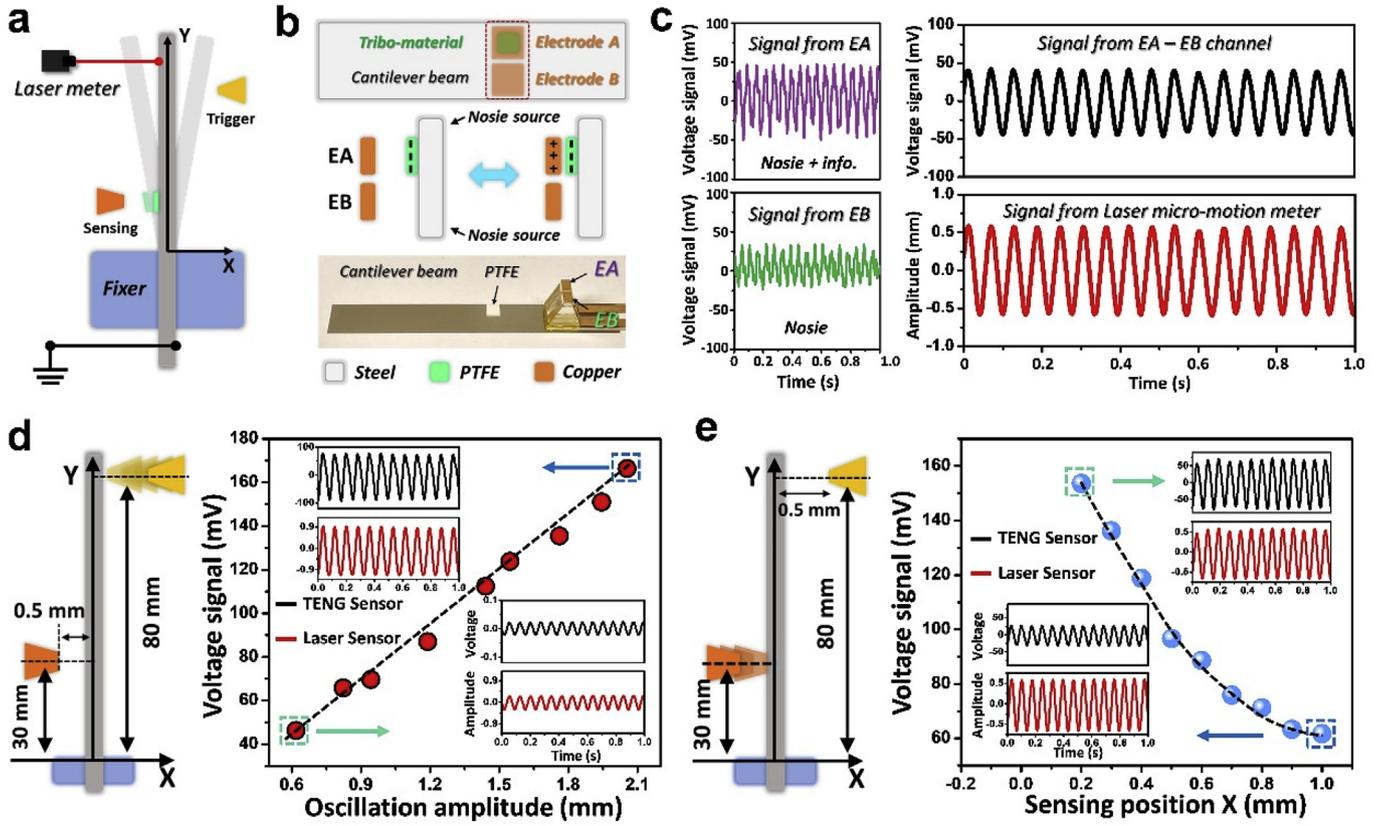
Fig. 4. Performance of the real-time oscillation-monitoring sensor (ROS). a) Scheme of the experimental configuration. **b)** Structure of the single electrode mode triboelectric nanogenerator based micro-motion sensing component. **c)** Electric signals from EA, EB and EA-EB, and the oscillation amplitude captured by the laser micro-motion meter. **d)** Electric signal of the ROS under various oscillation amplitudes. **e)** Electric signal of the ROS under various sensing position X.

Experimental data show that the ROS has the characteristics of linear sensing and high sensitivity. In addition, changing the X position of ROS can further improve the output signal level. The reason is that, with a smaller distance between the electrode and tribo-layer, the edge effect of this capacitor type device would be reduced, and the same gap variation would bring about a bigger effect on the capacitance, thus, a higher signal level and sensitivity can be achieved (Fig. 4e).

2.5. Application demonstration of the motion-triggered cantilever system

As a high-frequency oscillation cantilever, we demonstrate that the MC can be used for a periodical electric switch driven by a mechanical trigger. During the oscillation process of the cantilever, the LEDs located at the double sides of the cantilever beam will be powered separately, and the flash frequency of LEDs is consistent with the oscillation frequency of the cantilever. Fig. 5a presents the structure of this electric switch and the lighted LEDs (The process is shown in Video S6). The LED's flash frequency with different electric switch lengths is measured by the photoelectric detector, shown in Fig. 5b, in which the pulse voltage of the red LED is one-by-one with that of the purple LED, and the high-frequency pulse voltage corresponds to the short cantilever electric switch. On the basis of the MC integrated with ROS, a self-powered micro-weighting system is demonstrated, illustrated in Fig. 5c. In this demo, the mechanical energy generated by a random hand sliding at low-frequency has been converted into electricity and is then used to actuate the cantilever, the resonant frequency of cantilever with length L, width W, and thickness T is [39,40].

$$f_n = \frac{v_n^2}{2\pi} \frac{1}{L^2} \sqrt{\frac{D}{m}}$$

where v_n is the eigenvalue calculated from the nth positive root of

$1 + \cos(v_n)\cosh(v_n) = 0$, and n is a positive integer, D is the bending modulus in per unit width and m is the mass per unit area of the cantilever. Considering a small mass (Δm) loaded at the tip of the cantilever as schematically shown in Fig. 5c, the resonance frequency changes into [10,40].

$$f_n' = \frac{v_n'^2}{2\pi} \sqrt{\frac{K}{M + \Delta m}}$$

$v_n^2 = v_n'^2 \sqrt{3/0.236}$, effective spring constant $K = 3DW/L^3$ effective mass at the cantilever tip $M = 0.236mWL$, the resonance frequency shift Δf_n is

$$\Delta f_n = f_n - f_n' \cong \frac{1}{2} f_n \frac{\Delta m}{M}$$

For a given cantilever, Young's modulus E and density ρ is fixed, thus, the resonance frequency shift in per unit loaded mass depends only on the length and width of the cantilever and eigenvalues as

$$\frac{\Delta f_n}{\Delta m} \propto \frac{V_n^2}{WL^3}$$

In this work, only the first order oscillation in a transverse mode is considered. Therefore, for a cantilever with 40 mm length, 5 mm width, and 100 μm thickness, the frequency shift varies linearly with the loaded mass. The resonance frequency shift in per unit loaded mass is inversely proportional to the cantilever length. The detailed theoretical analysis process is shown in the Supplementary note. Fig. 5d exhibits the experimental results about frequency shift depending on loaded mass, which agrees with the above theoretical analysis. And then, objects with 5.5 mg, 8.7 mg, and 12.6 mg are weighed by the system. By just moving the slider of TENG, the weight can be obtained (Fig. 5e and Video S7). These results demonstrate that the self-powered micro-weighing system combing MC and ROS can be triggered by a sliding movement, with great accuracy for object mass weighing.
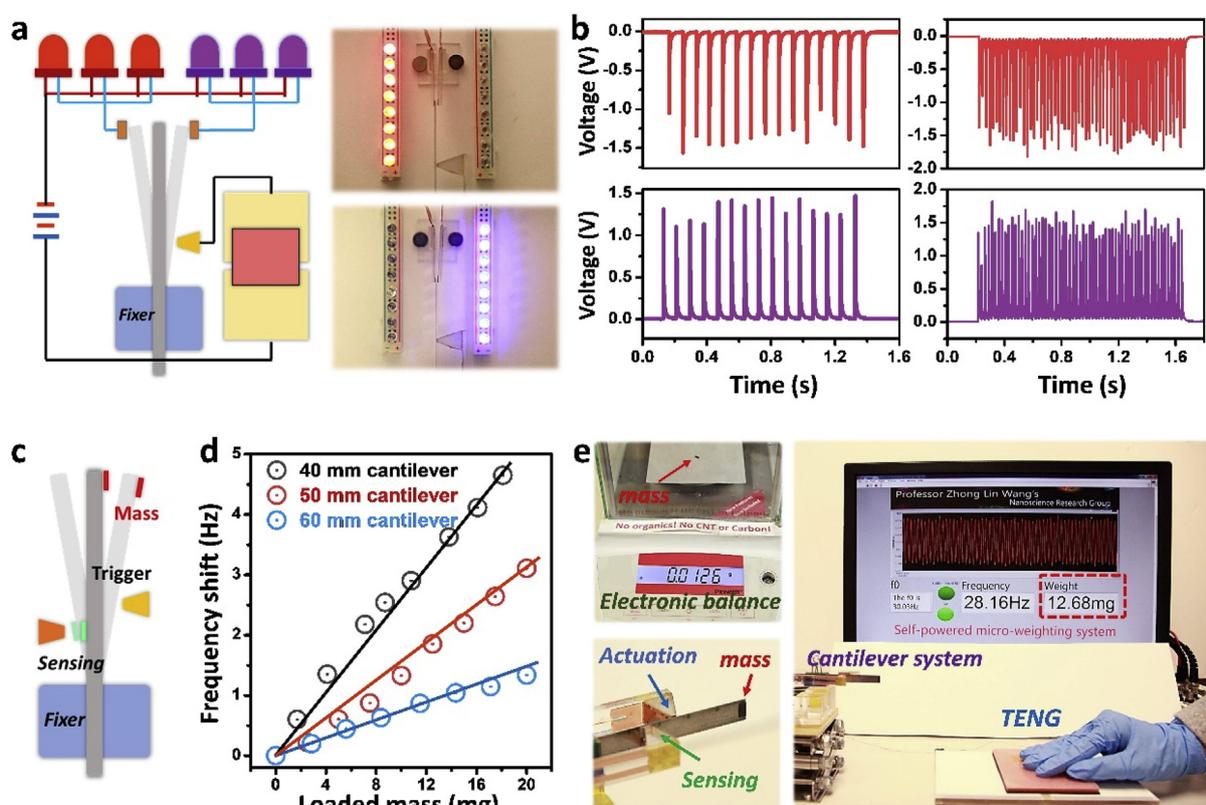
Fig. 5. Application of the triboelectric nanogenerator actuation and sensing integrated cantilever system. a) Demonstration of the cantilever beam as a motion-triggered high-frequency electric switch. **b)** Electric signals from the photoelectric sensors when using the low and high eigenfrequency cantilever, respectively. **c)** Structural scheme of the self-powered micro-weighting system. **d)** Linear relationship between frequency shift and loaded mass weight. **e)** Demonstration of the micro-mass weighing using the actuation and sensing integrated cantilever system.

Supplementary video related to this article can be found at https://doi.org/10.1016/j.nanoen.2019.103920.

3. Conclusion

In summary, we introduced an MC integrating with ROS system based on TENG technology. Utilizing the periodically built and neutralized high DC voltage during operating the freestanding mode TENG, a low-frequency mechanical motion can be converted to the high-frequency and regular oscillation up to 100 Hz. Significantly different from AC actuation that is selective to frequency, this DC voltage actuation strategy can perform all cantilever systems. And the oscillation performances of the MC were investigated in detail at different structural parameters of the cantilever system. Additionally, assembled with a single electrode mode TENG, the integrated self-powered ROS exhibits an ultra-high sensitivity (223 mV/mm compared with 72 mV/mm for laser micro-motion meter), indicating that this ROS can replace the laser micro-motion sensor to real-time monitoring of the oscillation of the cantilever. Furthermore, a self-powered micro-weighing system based on MC and ROS was demonstrated for measuring the object at the tip of the cantilever with milligram accuracy. This study provides a new strategy to actuate the cantilever by motion trigger without an external power source and shows the great potential in applying the TENG technology to both power supply and sensing in MEMS applications.

4. Materials and methods

4.1. Fabrication of the motion-triggered cantilever beam (MC)

MC consists of three parts, a cantilever beam, a trigger electrode, and an exciting source. For the cantilever beam, first, the commercial

stainless steel sheet (25, 50, 75, 100 μm thickness) was cut into strip shape. Second, the well-cut cantilever was bound to a copper wire with a conductive epoxy after cleansing the surface coating and oxide. And then, the cantilever was rigidly clamped at one end with a plastic fixture. The lengths of the cantilevers varied from 20 mm to 80 mm by changing the clamp position. Copper coated trapezoidal blocks with different width (0.1, 0.5, 1.0, 1.5, 2.0, 3.0, 5.0 mm) work as the trigger electrodes. For the exciting source, a freestanding mode triboelectric nanogenerator (TENG) was employed to provide high DC voltage. Typically, two acrylic sheets (110 mm × 175 mm, 100 mm × 80 mm) were shaped by a laser cutter as the substrate. Two thin Al films with dimensions of 110 mm × 80 mm were attached to the bigger substrate with a 5 mm gap. Then, a PTFE layer was covered on the two Al electrodes. A nylon film was bound to the small substrate to work as the tribo-positive slider. Lastly, conducting wires were connected with the two electrodes for the subsequent electrical measurement.

4.2. Fabrication of the real-time oscillation-monitoring sensor (ROS)

Based on the single electrode mode TENG structure, a PTFE film (1 mm × 1 mm) was attached to the cantilever to work as the tribo-negative layer. The corresponding electrode (EB) was fabricated on a trapezoidal block. Another electrode (EA) was introduced in its adjacent position. The sensing electrode of ROS was located inside of the cantilever, while the trigger electrode of MC was located on the other side of the cantilever.

4.3. Experimental setup for quantitative measurement

The oscillation process of the cantilever was characterized by a high-speed camera. A high voltage source (Series 230) was used to

supply a stable DC voltage to actuate the cantilever, and its oscillation was monitored by a laser micro-motion sensor (Panasonic HG-C1100). A programmable electrometer (Keithley 6514) was adopted to test the output performance of MC and ROS. COMSOL MULTIPHYSICS was employed for the potential and electric field distribution simulation.

Author contributions

J. Chen, H. Y. Guo and Z. Y. Wu contributed equally to this work.

Conflicts of interest

The authors declare no conflict of interest.

Acknowledgements

Appendix A. Supplementary data

Supplementary data to this article can be found online at https://doi.org/10.1016/j.nanoen.2019.103920.

References

[1] T. Emerson, A. Lozzi, H. Bai, J. Manimala, Dynamic characterization and control of a metamaterials-inspired Smart composite, Proc. ASME Conf. Smart Mater. Adapt. Struct. Intell. Syst. 1 (2018) V001T001A005.

[2] S. Liu, A. Davidson, Q. Lin, Simulation studies on nonlinear dynamics and chaos in a MEMS cantilever control system, J. Micromech. Microeng. 14 (2004) 1064–1073.

[3] W.J. Choi, Y. Jeon, J.H. Jeong, R. Sood, S.G. Kim, Energy harvesting MEMS device based on thin film piezoelectric cantilevers, J. Electroceram. 17 (2006) 543–548.

[4] A. Boisen, J. Thaysen, H. Jensenius, O. Hansen, Environmental sensors based on micromachined cantilevers with integrated read-out, Ultramicroscopy 82 (2000) 11–16.

[5] Y.H. Wang, C.Y. Lee, C.M. Chiang, A MEMS-based air flow sensor with a free-standing micro-cantilever structure, Sensors 7 (2007) 2389–2401.

[6] P. Ivaldi, J. Abergel, M.H. Matheny, L.G. Villanueva, R.B. Karabalin, M.L. Roukes, P. Andreucci, S. Hentz, E. Defaÿ, 50 nm thick AlN film-based piezoelectric cantilevers for gravimetric detection, J. Micromech. Microeng. 21 (2011) 085023.

[7] P. Xu, X. Li, H. Yu, T. Xu, Advanced nanoporous materials for micro-gravimetric sensing to trace-level bio/chemical molecules, Sensors 14 (2014) 19023–19056.

[8] S. Saadon, O. Sidek, A review of vibration-based MEMS piezoelectric energy harvesters, Energy Convers. Manag. 52 (2011) 500–504.

[9] H.S. Kim, J.-H. Kim, J. Kim, A review of piezoelectric energy harvesting based on vibration, Int. J. Precis. Eng. Manuf. 12 (2011) 1129–1141.

[10] B.N. Johnson, R. Mutharasan, Biosensing using dynamic-mode cantilever sensors: a review, Biosens. Bioelectron. 32 (2012) 1–18.

[11] M. Sanati, A. Sandwell, H. Mostaghimi, S.S. Park, Development of nanocomposite-based strain sensor with piezoelectric and piezoresistive properties, Sensors 18 (2018) 3789.

[12] S. Shi, Q. Yue, Z. Zhang, J. Yuan, J. Zhou, X. Zhang, S. Lu, X. Luo, C. Shi, H. Yu, A self-powered engine health monitoring system based on L-shaped wideband piezoelectric energy harvester, Micromachines (Basel) 9 (2018) 629.

[13] S.V. Pham, L.J. Kauppinen, M. Dijkstra, H.A.G.M. van Wolferen, R.M. de Ridder, H.J.W.M. Hoekstra, Read-out of cantilever bending with a grated waveguide optical cavity, IEEE Photonics Technol. Lett. 23 (2011) 215–217.

[14] N. Noeth, S.S. Keller, A. Boisen, Integrated cantilever-based flow sensors with tunable sensitivity for in-line monitoring of flow fluctuations in microfluidic systems, Sensors 14 (2013) 229–244.

[15] S.M. Firdaus, I.A. Azid, O. Sidek, K. Ibrahim, M. Hussien, Enhancing the sensitivity of a mass-based piezoresistive micro-electro-mechanical systems cantilever sensor, Micro & Nano Lett. 5 (2010) 85.

[16] Z.L. Wang, Triboelectric nanogenerators as new energy technology for self-powered systems and as active mechanical and chemical sensors, ACS Nano 7 (2013) 9533–9557.

[17] F.-R. Fan, Z.-Q. Tian, Z. Lin Wang, Flexible triboelectric generator, Nano Energy 1 (2012) 328–334.

[18] J. Chen, H. Guo, G. Liu, X. Wang, Y. Xi, M.S. Javed, C. Hu, A fully-packaged and robust hybridized generator for harvesting vertical rotation energy in broad frequency band and building up self-powered wireless systems, Nano Energy 33 (2017) 508–514.

[19] Y. Zi, H. Guo, Z. Wen, M.H. Yeh, C. Hu, Z.L. Wang, Harvesting low-frequency (< 5

Hz) irregular mechanical energy: a possible killer application of triboelectric nanogenerator, ACS Nano 10 (2016) 4797–4805.

[20] J. Liu, W. Tang, X. Meng, L. Zhan, W. Xu, Z. Nie, Z. Wang, Improving the performance of the mini 2000 mass spectrometer with a triboelectric nanogenerator electrospray ionization source, ACS Omega 3 (2018) 12229–12234.

[21] A. Li, Y. Zi, H. Guo, Z.L. Wang, F.M. Fernandez, Triboelectric nanogenerators for sensitive nano-coulomb molecular mass spectrometry, Nat. Nanotechnol. 12 (2017) 481–487.

[22] J. Cheng, W. Ding, Y. Zi, Y. Lu, L. Ji, F. Liu, C. Wu, Z.L. Wang, Triboelectric microplasma powered by mechanical stimuli, Nat. Commun. 9 (2018) 3733.

[23] J. Chen, H. Guo, J. Zheng, Y. Huang, G. Liu, C. Hu, Z.L. Wang, Self-powered triboelectric micro liquid/gas flow sensor for microfluidics, ACS Nano 10 (2016) 8104–8112.

[24] X. Li, M.H. Yeh, Z.H. Lin, H. Guo, P.K. Yang, J. Wang, S. Wang, R. Yu, T. Zhang, Z.L. Wang, Self-powered triboelectric nanosensor for microfluidics and cavity-confined solution chemistry, ACS Nano 9 (2015) 11056–11063.

[25] Z.L. Wang, Triboelectric nanogenerators as new energy technology and self-powered sensors - principles, problems and perspectives, Faraday Discuss 176 (2014) 447–458.

[26] Z.L. Wang, On maxwell's displacement current for energy and sensors: the origin of nanogenerators, Mater. Today 20 (2017) 74–82.

[27] D. Bhatia, W. Kim, S. Lee, S.W. Kim, D. Choi, Triboelectric nanogenerators for optimally scavenging mechanical energy with broadband vibration frequencies, Nano Energy 33 (2017) 515–521.

[28] L.B. Huang, G. Bai, M.C. Wong, Z. Yang, W. Xu, J. Hao, Magnetic-assisted non-contact triboelectric nanogenerator converting mechanical energy into electricity and light emissions, Adv. Mater. 28 (2016) 2744–2751.

[29] X. Pu, H. Guo, J. Chen, X. Wang, Y. Xi, C. Hu, Z.L. Wang, Eye motion triggered self-powered mechnosensational communication system using triboelectric nanogenerator, Sci. Adv. 3 (2017) e1700694.

[30] Q. Zheng, B. Shi, F. Fan, X. Wang, L. Yan, W. Yuan, S. Wang, H. Liu, Z. Li, Z.L. Wang, In vivo powering of pacemaker by breathing-driven implanted triboelectric nanogenerator, Adv. Mater. 26 (2014) 5851–5856.

[31] J. Tian, R. Shi, Z. Liu, H. Ouyang, M. Yu, C. Zhao, Y. Zou, D. Jiang, J. Zhang, Z. Li, Self-powered implantable electrical stimulator for osteoblasts' proliferation and differentiation, Nano Energy 59 (2019) 705–714.

[32] Z. Wen, J. Chen, M.-H. Yeh, H. Guo, Z. Li, X. Fan, T. Zhang, L. Zhu, Z.L. Wang, Blow-driven triboelectric nanogenerator as an active alcohol breath analyzer, Nano Energy 16 (2015) 38–46.

[33] S. Lv, B. Yu, T. Huang, H. Yu, H. Wang, Q. Zhang, M. Zhu, Gas-enhanced triboelectric nanogenerator based on fully-enclosed structure for energy harvesting and sensing, Nano Energy 55 (2019) 463–469.

[34] Z. Liu, Z. Zhao, X. Zeng, X. Fu, Y. Hu, Expandable microsphere-based triboelectric nanogenerators as ultrasensitive pressure sensors for respiratory and pulse monitoring, Nano Energy 59 (2019) 295–301.

[35] T.Q. Trung, N.E. Lee, Flexible and stretchable physical sensor integrated platforms for wearable human-activity monitoring and personal healthcare, Adv. Mater. 28 (2016) 4338–4372.

[36] J. Jang, J. Lee, J.H. Jang, H. Choi, A triboelectric-based artificial basilar membrane to mimic cochlear tonotopy, Adv. Healthc. Mater. 5 (2016) 2481–2487.

[37] H.Y. Guo, X.J. Pu, J. Chen, Y. Meng, M.H. Yeh, G.L. Liu, Q. Tang, B.D. Chen, D. Liu, S. Qi, C.S. Wu, C.G. Hu, J. Wang, Z.L. Wang, A highly sensitive, self-powered triboelectric auditory sensor for social robotics and hearing aids, Sci. Rob. 3 (2018) eaat2516.

[38] J.A. Malecki, Linear decay of charge in electrets, Phys. Rev. B 59 (1999) 9954–9960.

[39] J.W. Yi, W.Y. Shih, W.-H. Shih, Effect of length, width, and mode on the mass detection sensitivity of piezoelectric unimorph cantilevers, J. Appl. Phys. 91 (2002) 1680–1686.

[40] A. Boisen, S. Dohn, S.S. Keller, S. Schmid, M. Tenje, Cantilever-like micro-mechanical sensors, Rep. Prog. Phys. 74 (2011) 036101.

Jie Chen received her B. S. degree in Applied Physics from Chongqing University, China in 2015. Now she is a Ph.D. candidate in the field of Physics, Chongqing University. Her current research interest is triboelectric nanogenerator.

Hengyu Guo received his B. S. and Ph.D. degree in Applied Physics from Chongqing University, China. Now he is a postdoctoral fellow in Georgia institute of technology, Zhong Lin Wang' group. His current research interest is triboelectric nanogenerator based energy and sensor systems.
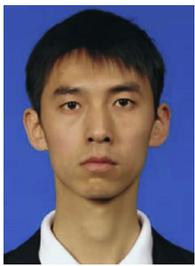
Chenguo Hu is a professor of physics in Chongqing University and the director of Key Lab of Materials Physics of Chongqing Municipality. She received her Ph.D. in Materials from Chongqing University in 2003. Her research interests include methodology of synthesizing functional nanomaterials, investigation of morphology and size dependent physical and chemical properties of nanomaterials, and design and fabrication of electronic devices, such as nanogenerators and sensors.

Zhiyi Wu received Ph.D. degree in Instrument Science and Technology from Chongqing University, in 2013. He is now a Visiting Scientist in Professor Zhong Lin Wang's group at Georgia Institute of Technology. His current research focuses on the Nanoenergy and Nano sensors.

Zhong Lin Wang received his Ph.D. from Arizona State University in physics. He now is the Hightower Chair in Materials Science and Engineering, Regents' Professor, Engineering Distinguished Professor and Director, Center for Nanostructure Characterization, at Georgia Tech. Dr. Wang has made original and innovative contributions to the synthesis, discovery, characterization and understanding of fundamental physical properties of oxide nanobelts and nanowires, as well as applications of nanowires in energy sciences, electronics, optoelectronics and biological science. His discovery and breakthroughs in developing nanogenerators established the principle and technological road map for harvesting mechanical energy from environment and biological systems for powering personal electronics. His research on self-powered nanosystems has inspired the worldwide effort in academia and industry for studying energy for micro-nano-systems, which is now a distinct disciplinary in energy research and future sensor networks. He coined and pioneered the field of piezotronics and piezophototronics by introducing piezoelectric potential gated charge transport process in fabricating new electronic and optoelectronic devices. Details can be found at: http://www.nanoscience.gatech.edu.

Guoqiang Xu received his B.Eng. degree from Tsinghua University in 2013. Now he worked with Prof. Yunlong Zi at CUHK as a Ph.D. student in 2018. His research interests mainly focus on basic theories of TENG, energy harvesting and sensors.

Yunlong Zi received his B.Eng. degree from Tsinghua University in 2009. He received his Ph.D. degree from Purdue University in 2014. After his graduate study, he worked as a Postdoctoral Fellow at Georgia Institute of Technology during 2014–2017. Dr. Zi joined the Chinese University of Hong Kong as an Assistant Professor in November 2017, as the founder of the Nano Energy and Smart System laboratory